Hybrid PV-Reheat Thermal Power System Automatic Generation Control Using PIDD Controller Based on Hippopotamus Algorithm

Jirawat Riyawong, Sitthisak Audomsi, Worarat Phakditha, Chatmongkol Areeyat, Kunakorn Pakdeesuwan, Palapol Sawatphol, Supakorn Ukumphan, Worawat Sa-ngiamvibool, Supannika Wattana*

Faculty of Engineering, Mahasarakham University, Maha Sarakham, 44150, Thailand

***Corresponding authors**: *supannika.w@msu.ac.th*
https://doi.org/10.55674/ias.v14i3.263235

Received: 20 June 2025 ; **Revised:** 22 August 2025 ; **Accepted:** 30 September 2025 ; **Available online:** 20 October 2025

Abstract

This paper examines load frequency control, an essential element of the power system that ensures frequency stability and enhances reliability, particularly in contemporary power systems incorporating renewable energy sources like photovoltaic power plants (PV) in two-area configurations and reheat thermal power plants. This research examines and contrasts metaheuristic algorithms for optimizing the settings of two sets of proportional-integral-double derivative (PIDD) controllers in regulating a two-area power plant to enhance system response. The comparative analysis of the results employed Hippopotamus algorithm (HO), Particle swarm optimization (PSO), Water cycle algorithm (WCA), and Grey wolf optimizer (GWO) to evaluate performance based on the ITAE objective function, which encompasses Overshoot, Undershoot, and Settling Time. The experimental results indicate that HO provides the lowest ITAE objective function values compared to other algorithms, exhibiting exceptional responsiveness, stability, and less settling time. This suggests that HO is an appropriate technique to be used in load frequency control for a two-area PV-reheat thermal power system.

Keywords: Load frequency control; Hybrid PV-reheat thermal system; Hippopotamus algorithm; PIDD

1. Introduction

The power system is a complex system that maintains the stability of the power supply to be constant and sufficient because the power system is a fluctuating and uncertain system, such as sudden load deviations, which cause changes in the system frequency. Inadequate control may result in issues such as power breakdown [1]. The most ideal approach is load frequency control (LFC) [2]. Given the constant fluctuations in load within the power system, it is crucial to sustain equilibrium between generation and consumption. The primary objective of LFC is to ensure that the frequency and power of the interconnecting lines remain within the required range to address fluctuations in frequency and other disturbances [3, 4].

In recent years, hybrid power systems integrating photovoltaic (PV) generation with thermal units, particularly reheat thermal generators, have been increasingly studied. Several works have investigated the role of PV–thermal systems in LFC design. For instance, Abd-Elazim and Ali [5] introduced the firefly algorithm (FA) for optimal tuning of controllers in a PV–thermal hybrid system, Tomy and Prakash [6] presented an LFC framework incorporating MPPT for a PV system connected to a thermal generator. More studies have applied optimization methods such as modified whale optimization [7], black widow optimization [8], and salp swarm algorithm with energy storage to improve the stability of PV–reheat hybrid configurations [9]. However, none of these studies have considered the Hippopotamus Optimization algorithm in PV–reheat thermal hybrid systems.

Compared with traditional single-source systems, PV-reheat thermal hybrids pose additional challenges. PV generation is highly intermittent and uncertain, depending on solar irradiance and temperature, which leads to rapid and unpredictable frequency and tie-line power deviations. In contrast, reheat thermal units, although stable and equipped with high inertia, suffer from sluggish responses due to reheater time constants and delays. This mismatch between fast PV fluctuations and slow thermal dynamics introduces strong nonlinearities, making LFC design more complex than in conventional thermal-only or hydro-only systems [8 – 10]. Therefore, advanced and robust optimization-based controllers are required to achieve reliable frequency regulation in such hybrid systems.

The control system typically employs standard controllers. Classical controllers, such as proportional-integral (PI) or proportional-integral derivative (PID), are extensively utilized in the design and regulation of LFC in multi-area power systems. Conversely, the dynamic characteristics of these classical controllers exhibit considerable prolonged settling times and oscillations [11]. Consequently, several novel controllers have lately been implemented in LFC, including the integral-double derivative (IDD) controller [12] and the PIDD controller [12 – 14]. The implementation of PIDD controllers, an enhancement of the PID controller through the incorporation of a derivative component, enhances response efficiency in the power system. To modify the controller parameters, the following calculating procedures are necessary [15]. Owing to the system's non-linear characteristics and the challenge of optimization, numerous studies have employed optimization methods to refine the controller parameters. In this research, a new algorithm that has been developed and not much research has applied, the Hippopotamus Algorithm (HO) [16] is introduced. In addition, other algorithms are used to compare the efficiency of HO, which include PSO [17], WCA [18], and GWO [19] to tune the parameters of the PIDD controller mentioned above. The efficiency comparison takes the results of all algorithms into consideration, using the integral time-weighted absolute error (ITAE) objective function to evaluate the efficiency by considering the values of overshoot, undershoot, and settling time. While previous research has utilized FA [5], MWOA [7], BWOA [8], and SSA [9] for PV–thermal systems, none have applied HO for PV–reheat thermal systems. The proposed HO-based PIDD controller is therefore novel, as HO demonstrates faster convergence, stronger capability to avoid local optima, and better balance between exploration and exploitation compared to earlier algorithms.

2. Materials and Methods

2.1 System modeling

The present study presents a hybrid two-area power system consisting of a photovoltaic system and a thermal-reheat system , where the PV system is placed in area 1 of the system layout, while the thermal-reheat system is designed to be placed in area 2 of the system layout, and the system layout is shown in Fig. 1.[20]

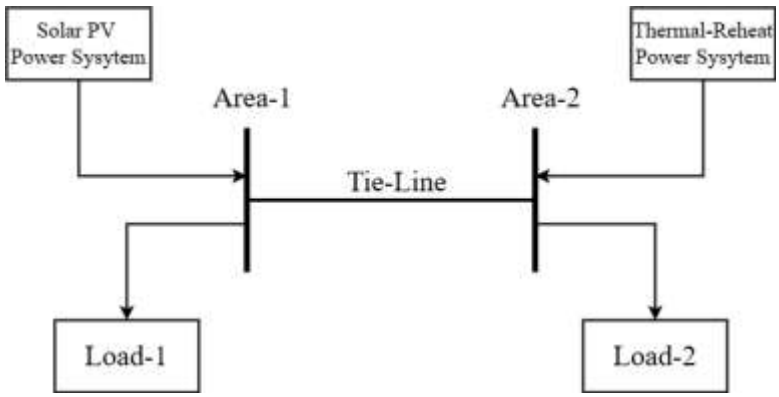

Fig. 1 Schematic diagram of power system.

2.1.1 Photovoltaic system

In the system studied in this research, the photovoltaic (PV) system is used as a power generation source in Area 1 of the two-area hybrid system and is connected to Area 2, which is a reheat thermal power system. The solar cell model used in the simulation consists of a solar intensity-dependent current source connected in parallel with a diode and a small contact resistor

connected in series with the terminals of the solar cell that show in Fig. 2. This structure appropriately reflects the physical behavior of the solar cell panel. The electrical power and voltage obtained from PV panels will change all the time depending on other factors such as solar radiation intensity (irradiance) and environmental temperature. To maximize the efficiency of power generation at any time, Maximum Power Point Tracking (MPPT) is used in conjunction with the PV system. The MPPT algorithm modifies the operating point of the photovoltaic array in reaction to variations in solar irradiation and temperature, thereby guaranteeing that the photovoltaic system functions at peak efficiency. Various MPPT methodologies have been introduced, such as perturb-and-observe and incremental conductance [21], fuzzy logic and hill-climbing techniques [6], mid-point tracking, and more recent AI-based approaches [20]. The MPPT will adjust the operation value of the Power Converter to suit the sunlight and temperature at that time so that the solar cell panel can supply the most energy. In the PV system, it consists of solar cell panel, MPPT, DC-AC converter (Inverter) and filter, which can be represented by the transfer function as eq. (1). [6, 22 – 24]

$$G_{PV}(s) = \frac{-18s+900}{s^2+100s+50} \tag{1}$$

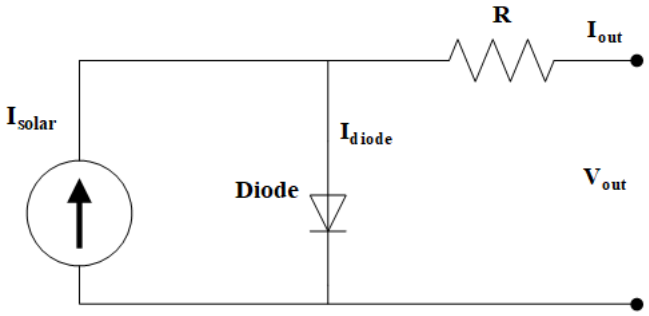

Fig. 2 Solar equivalent circuit.

2.1.2 Thermal-reheat power system

Thermal power system with reheat turbine in Area 2 consists of four main parts: the governor, turbine, reheater, and power system, where each transfer function is explained as follows [25]. The transfer function (TF) of the governor is described in eq. (2); [6, 22]

$$G_g(s) = \frac{K_g}{sT_t + 1} \tag{2}$$

The TF of the turbine is described in eq. (3);

$$G_t(s) = \frac{K_t}{sT_t+1} \tag{3}$$

The TF of the reheater is described in eq. (4);

$$G_r(s) = \frac{sK_rT_r}{sT_r+1} \tag{4}$$

The TF of the power system is described in eq. (5);

$$G_{ps}(s) = \frac{K_{ps}}{sT_{ps}+1} \tag{5}$$

The parameters for the modeling of the hybrid PV–reheat thermal power system are as follows. The power system gain is Kps = 120 Hz pu^{-1}.MW, and the time constant is τps = 20 s. The turbine is modeled with a time constant of τt = 0.30 s, while the governor has a time constant of τg = 0.08 s. The reheater is represented with a gain of Kr = 0.33 Hz/pu.MW and a time constant of τr = 10 s. The two areas are interconnected by a tie-line with synchronizing coefficient $2\pi T12$ = 0.545 pu.MW Hz^{-1}. The frequency bias factor is set as B = 0.80 pu.MW Hz^{-1}, and the speed regulation parameter is R = 2.50 Hz pu^{-1}.MW.

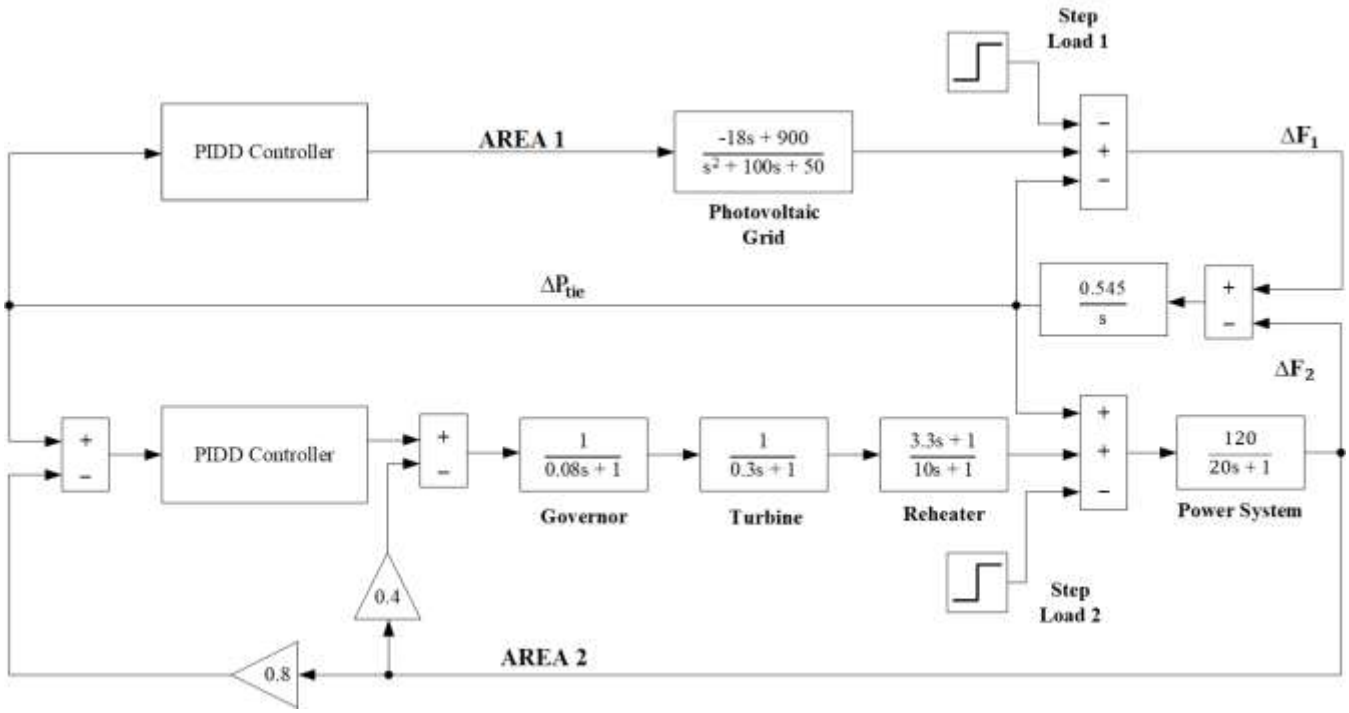

Fig. 3 Two-area hybrid system.

The two control areas are interconnected through a tie-line that enables power exchange between them. The tie-line power deviation is represented in eq. (6);

$$\Delta P_{tie}(s) = \frac{2\pi T_{12}}{s}\left[\Delta F_1(s) - \Delta F_2(s)\right] \tag{6}$$

Where ΔF_1 and ΔF_2 denote the frequency deviations of Area-1 and Area-2, respectively. In the present study, the synchronizing coefficient is directly set as $2\pi T_{12} = 0.545$ pu.MW Hz^{-1}, this parameter determines the sensitivity of tie-line power flow to frequency differences between the two areas.

2.2 PIDD controller

This research has applied a Proportional-Integral-Double Derivative (PIDD) controller to replace PI or PID controller for the purpose of increasing the accuracy of frequency control, reducing oscillation and reducing setting time. The structure of PIDD controller consists of three parameters: KP, KI and KDD, which can be written as a transfer function as eq. (7). It can also be written as a structural diagram, as in Fig. 4.

$$PIDD(s) = K_P + \frac{K_I}{s} + K_{DD}s^2 \tag{7}$$

The six parameters, K_p, K_i, and K_{dd}, of both controllers will be randomly selected or tuned by PSO, GWO, and HO to find the best result by considering the best value according to the objective function ITAE as eq. (8).

$$\text{Objective function}_{ITAE} = \int_0^T t \cdot \left(|\Delta F_1 + \Delta F_2 + \Delta P_{tie}|\right) \cdot dt \tag{8}$$

ITAE is selected as the objective function because it penalizes late-occurring errors more heavily than early ones, which promotes a faster damping of oscillations, expedited system response, and better steady-state accuracy. This makes ITAE particularly suitable for load frequency control in hybrid PV–reheat thermal systems, as it reflects both error minimization and dynamic stability. By minimizing ITAE, the controller inherently reduces overshoot, undershoot, and settling time, thereby indicating improved transient performance as well as stability. In this study, system stability under PIDD control is evaluated based on the ITAE criterion together with transient performance indices such as overshoot, undershoot, and settling time. A

system is regarded as stable when frequency deviations converge to zero, tie-line power deviations remain within the acceptable tolerance band, and no sustained oscillations are observed in the time-domain responses. The specified parameter search ranges for both controllers are specified as $-3 \leq K_{p1}, K_{i1}, K_{dd1}, K_{p1}, K_{i1}, K_{dd2} \leq 3$

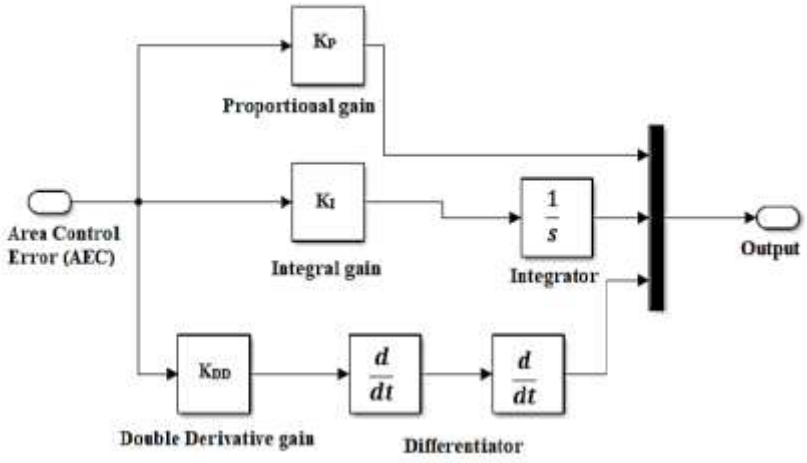

Fig. 4 Block diagram of PIDD controller.

2.3 Hippopotamus Algorithm (HO)

The Hippopotamus Algorithm (HO) was developed and described in detail by Mohammad Hussein Amiri et al. [16] It was derived from the natural behavior of hippopotamus by emulating three behaviors of hippopotamus, which are divided into Exploration Phase, Defense Phase and Escape Phase.

HO starts by specifying parameters such as population (N), number of iterations (T), problem size (dimension), and scope of variables. Then, randomize the initial position of hippopotamus in the area to be searched according to eq. (9)

$$x_{i,j} = lb_j + r \cdot (ub_j - lb_j), \; i = 1,2,\ldots,N, \; j = 1,2,\ldots,m \tag{9}$$

After randomizing the initial position, it calculates the fitness value by the objective function and selects the hippopotamus with the lowest fitness value (dominant hippopotamus) for updating the position.

In the Exploration Phase, the total population is divided in half. The first half of the population is updated with a new position, which simulates the behavior of hippopotamus in moving to water or food sources according to eq. (10) and eq. (11). After that, the position is updated again.

$$x_{i,j}^{Mhippo} = x_{i,j} + y_1 \cdot (D_{hippo} - I_1 x_{i,j}), \; \text{for } i = 1,2,\ldots,[\frac{N}{2}], \; j = 1,2,\ldots,m \tag{10}$$

$$x_{i,j}^{FBhippo} = x_{i,j} + h_1 \cdot (D_{hippo} - I_2 MG_i) \tag{11}$$

In the next phase, the Defense Phase, the remaining hippopotamus from the halving are selected to simulate escape behavior. Start by randomizing the position of predators using eq. (12). Then, find the new position of the hippopotamus according to eq. (13) and update the position. This phase is important because the process of randomizing the position of predators and the new position of hippopotamus helps avoid getting stuck in the local optima point by creating non-repeating points and randomizing the direction.

$$Predator_j = lb_j + \vec{r}8 \cdot (ub_j - lb_j), \; j = 1,2,\ldots,m \tag{12}$$

$$x_{i,j}^{HippoR} = \begin{cases} \overrightarrow{RL} \oplus Predator_j + \left(\frac{f}{(c - d \times \cos(2\pi g))}\right) \cdot \left(\frac{1}{\vec{D}}\right) & F_{Predator_j} < F_i \\ \overrightarrow{RL} \oplus Predator_j + \left(\frac{f}{(c - d \times \cos(2\pi g))}\right) \cdot \left(\frac{1}{2 \times \vec{D} + \vec{r}9.}\right) & F_{Predator_j} \geq F_i \end{cases} \quad (13)$$

$$for_i = [\frac{N}{2}] + 1, [\frac{N}{2}] + 2, \ldots, N \text{ and } j = 1,2,\ldots,m$$

When both phases are completed, the algorithm enters the Escape Phase, which focuses on fine-tuning and precise search by calculating the scope of new decision variables using eq. (14), which narrows the search scope by the number of iterations. After that, Hippopotamus is updated with a new position to obtain the optimal position or value in the range of the answer scope. After completing all three phases, the algorithm saves the value of the result of the hippopotamus with the best value, and at the end of the maximum iteration (T), the value of the hippopotamus with the best fitness value according to the objective function is displayed as the result of the algorithm.

$$lb\ local_j = \frac{lb_j}{t},\ ub\ local_j = \frac{ub_j}{t},\ t = 1,2,\ldots,T \quad (14)$$

Algorithm 1. Pseudo-code of HO

```
Start HO
Define an optimization problem
Set the number of population (N) and the maximum number of iteration (T)
Generate the initial position of population based on equation (8) and objective function evaluation for
this initial population
For t : 1 : T
    Update dominant hippopotamus position based on objective function value criterion
Phase 1: The hippopotamus position update in the river or pound
For i= 1 : N/2
    Calculate the new position for hippopotamus using equation (9)(10)
    Update position of hippopotamus
End for
Phase 2: Hippopotamus defense against predators
For i= 1 + N/2 : N
    Generate random position for predator using equation (11)
    Calculate the new position for hippopotamus using equation (12)
    Update the position of hippopotamus
End for
Phase 3: Hippopotamus Escaping from the Predator
Calculate new bounds of variables decision using equation (13)
For i = 1 : N
    Calculate the new position for hippopotamus
    Update the position of hippopotamus
  End for
Save the best candidate solution found so far.
End for
Output the best solution of the objective function found by HO
End HO
```

Fig. 5 Pseudo-code of HO.

Table 1 Parameter setting for solving problem.

Parameter	Value
Runs	10
Population	50
Iteration	50
Lower Bound	-3
Upper Bound	3

These parameters are included for all algorithms: HO, PSO (w_init = 1, wdamp = 0.99, c1 = 1.50, c2 = 2.00), WCA (Nsr = 4, dmax_init = 1e-8), and GWO for comparing results.

The stopping condition for all algorithms was a fixed maximum of 50 iterations. Performance evaluation was carried out over a 30-second simulation by the ITAE objective function together with transient indices, overshoot, undershoot, and settling time for ΔF1, ΔF2, and ΔPtie. To ensure robustness, the results were averaged over 10 independent runs.

3. Results and Discussions

Part of the experimental results This research presents an optimized controller. The controller parameters are adjusted by HO, PSO, WCA, and GWO for performance comparison. It is equipped with a thermal reheat turbine and a PV grid system. The response to a load change of 0.10 pu occurring in Area-2 (thermal reheat power system) at 0 s is simulated. The controller values are adjusted by HO, PSO, WCA, and GWO for efficiency comparison. The experiments are conducted through the program. MATLAB/Simulink on an Acer Predator laptop running 64-bit OS with an Intel® Core™ i9-13900HX processor and 32 GB DDR5 5600 MHz of RAM. The optimization procedure consisted of 10 runs with 50 populations and 50 iterations, as shown in Fig. 6.

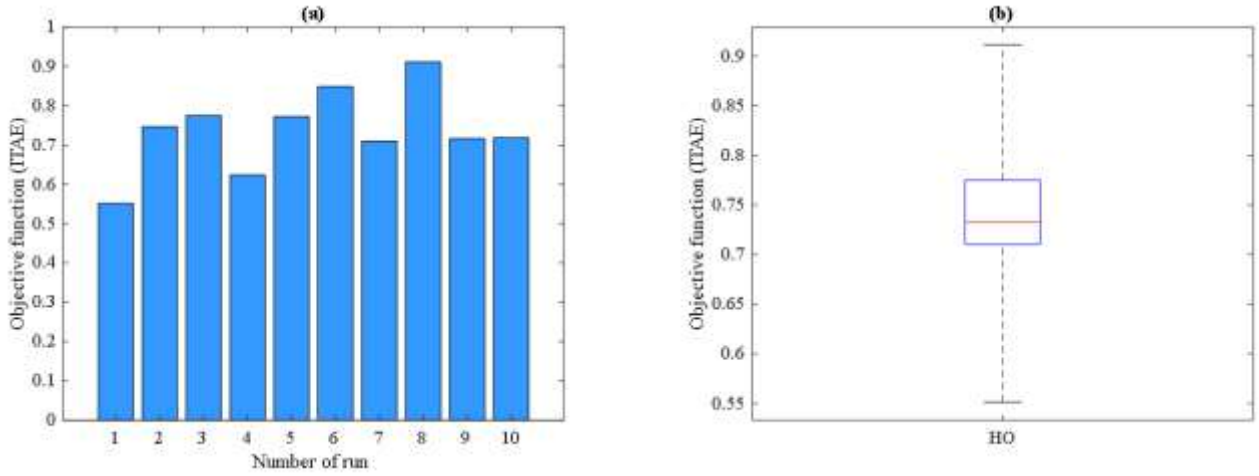

Fig. 6 (a) ITAE values for 10 runs and (b) Boxplot analysis for 10 runs.

From Fig. 6 showing that against the 10 test runs, the maximum value is 0.9111, the minimum value is 0.5512, and the average is 0.7374. Fig. 7 presents the test results producing the best objective function, with HO achieving an ITAE of 0.5512, in contrast to PSO (ITAE = 0.6759), WCA (ITAE = 0.6724), and GWO (ITAE = 0.6736). The gain values of both sets of controllers can be read in Table 2.

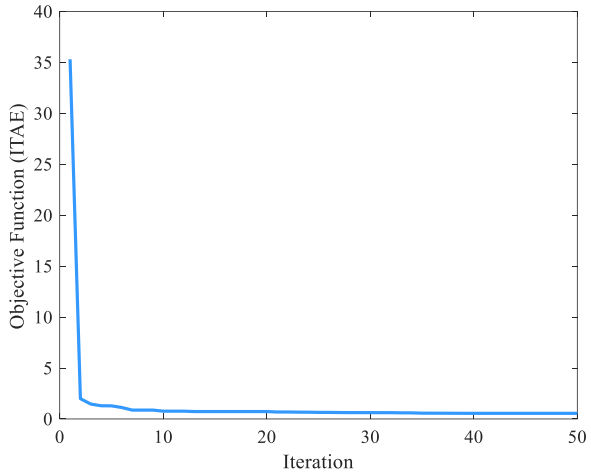

Fig. 7 Convergence curve of ITAE for best runs.

Table 2 Result of PIDD Controller Parameter.

Algorithm	Parameter					
	K_{P1}	K_{I1}	K_{DD1}	K_{P2}	K_{I2}	K_{DD2}
HO (Proposed)	-0.0750	-0.0126	-0.2011	-1.3272	-1.8173	-1.4406
PSO	-0.5689	-0.0452	-1.5179	-1.6831	-3	-1.3400
WCA	-0.5527	-0.0440	-1.4749	-1.6616	-3	-1.2634
GWO	-0.5022	-0.0412	-1.2411	-1.5521	-3	-1.1908

The results from the simulation displaying the frequency of both segments of the power system controlled by the tuned PIDD controller are shown in Fig. 7 for Area-1 (ΔF_1) and Fig. 8 for Area-2 (ΔF_2), together with the power in the tie-line presented in Fig. 9 (ΔP_{tie}) when Area 2 gets exposed to a 0.10 pu load at second 0.

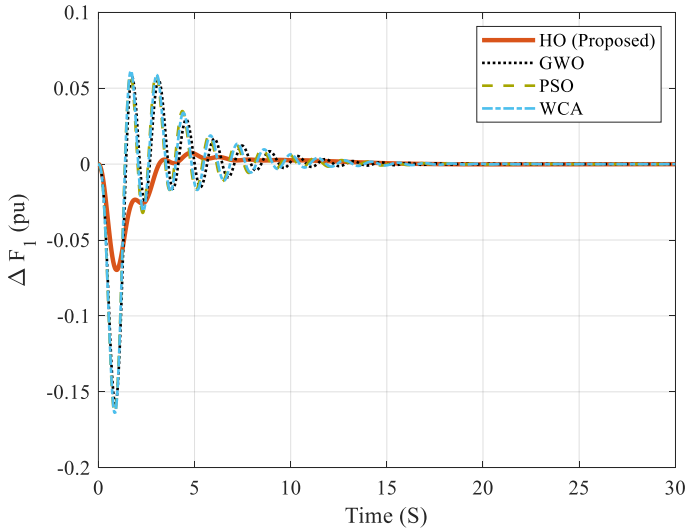

Fig. 8 Response of variation in Area 1.

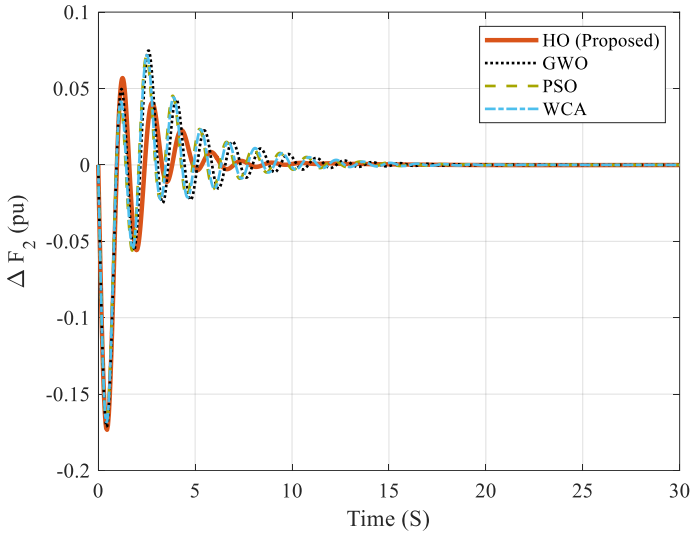

Fig. 9 Response of variation in Area 2.

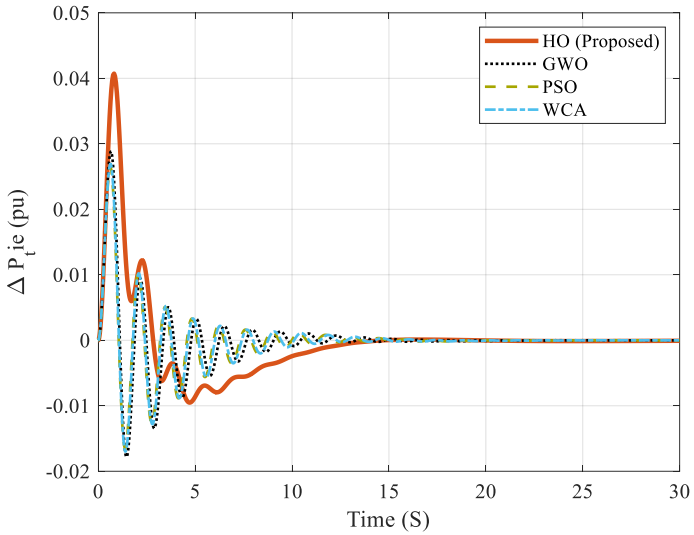

Fig. 10 Response of variation in tie-line.

From Fig. 8 – 10, it is observed that the frequency responses in Area-1 (ΔF_1), Area-2 (ΔF_2), and the tie-line power (ΔP_{tie}) exhibit noticeable oscillations following a 0.10 pu load change in Area-2. This transient imbalance arises from the different dynamics of the two power sources: Area-1, driven by PV generation, responds quickly but suffers from instability due to solar irradiance fluctuations, whereas Area-2, based on a thermal reheat system, has high inertia and a large reheater time constant, leading to slower responses with larger oscillation amplitudes. These contrasting characteristics cause significant initial fluctuations in tie-line power before the system gradually returns to equilibrium. Nevertheless, the HO-tuned PIDD controller demonstrates superior damping capability compared to the other algorithms. Specifically, the overshoot and undershoot of ΔF_1 are reduced to only 0.00738 and –0.06973, respectively, which are substantially lower than those of PSO (0.05929, –0.16404) and WCA (0.06143, –0.16411). The overshoot and undershoot of ΔF_1 is lowered to 0.00738 and –0.06973, respectively, much lower than those of PSO (0.05929, -0.16404) and WCA (0.06143, –0.16411). In addition, the HO-based controller obtains overshoot and undershoot values of 0.05684 and –0.17335 for ΔF_2, outperforming all other methods. The HO-tuned PIDD controller controls tie-line power deviation, producing an overshoot of 0.04072 and an undershoot of -0.00952, values nearly approaching zero, thereby signifying improved stability. Ultimately, in terms of settling time, the HO-based controller showed better performance, displaying 28.891 s for ΔF_1, 28.903 s for ΔF_2, and 29.178 s for ΔP_{tie}, while the other algorithms necessitate larger times, rang

Table 3 Result of ITAE values, settling time, Overshoot, Undershoot (ΔF_1, ΔF_2, ΔP_{tie}).

Algorithm	ITAE	(ΔF_1)			(ΔF_2)			(ΔP_{tie})		
		ST (S)	OS	US	ST (S)	OS	US	ST (S)	OS	US
HO	0.5512	28.891	0.0073	–0.0697	28.903	0.0568	–0.1734	29.178	0.04072	–0.0095
PSO	0.6759	29.692	0.0593	–0.1640	29.992	0.0710	–0.1672	29.921	0.02646	–0.0165
WCA	0.6724	29.965	0.0614	–0.1641	29.972	0.0718	–0.1684	29.808	0.02700	–0.0170
GWO	0.6736	29.904	0.0573	–0.15780	29.996	0.0750	–0.1713	29.895	0.02880	–0.0178

Table 3 shows the system response and results for the comparative analysis of ITAE, settling time (ST), overshoot (OS), and undershoot (US) values. In measuring the settling time, the step info function of MATLAB was used by setting the SettlingTimeThreshold parameter to 0.10, which means that the steady state of the system is allowed to vary within a ±10% range.

4. Conclusion

This research studies and defines a tuning technique for Proportional-Integral-Double-Derivative (PIDD) controller parameters using the Hippopotamus Optimization (HO) algorithm to control the load frequency of a dual-area power system integrating renewable energy sources from solar (photovoltaic – PV) and reheat thermal power plants. The results of the experiments indicate that HO is capable of modifying the controller parameters. In comparison to other algorithms, such as Particle Swarm Optimization (PSO), Water Cycle Algorithm (WCA), and Grey Wolf Optimizer (GWO), HO provides the lowest ITAE objective function value with excellent performance for overshoot, undershoot, and settling time. Specifically, HO achieved the best ITAE value of 0.5512, outperforming PSO (0.6759), WCA (0.6724), and GWO (0.6736). Moreover, HO shown the most fastest settling times, with 28.891 s for ΔF_1, 28.903 s for ΔF_2, and 29.178 s for ΔP_{tie}. Overshoot values were reduced to 0.00738 for ΔF_1 and 0.05684 for ΔF_2. Undershoot decreased to -0.06973 for ΔF_1 and -0.00952 for ΔP_{tie}. HO has the ability to find the answer that comes from imitating the behavior of a hippopotamus, which has a flexible exploration and answer-finding process that avoids local optima and can find good answers. However, in terms of answer-finding time, it is quite slow because of the direct behavior of hippopotamus, which is slow in some cases. This study represents the first application of the HO algorithm to optimize a PIDD controller for a hybrid PV-reheat thermal power system. In conclusion, the results indicate that the PIDD, optimized using the HO framework, attains the lowest ITAE while facilitating expedited settling, reduced overshoot, and minimal undershoot, which has excellent potential to improve the efficiency of frequency control systems in power systems with various energy sources and complex systems, both in terms of response speed and accuracy and stability of the system under uncertain conditions.

Acknowledgements

The researcher expresses appreciation to Professor Dr. Worawat Sa-ngiamvibool and Associate Professor Dr. Supannika Wattana for their guidance, sharing of knowledge, and support throughout this study project. Grateful acknowledgment is also extended to Mahasarakham University for providing the facilities that were necessary for working on this research.

References

[1] P. Kundur, Power system stability, in: Power System Stability and Control, vol. 10(1) (2007) 7–1.

[2] O. I. Elgerd, Electric Energy Systems Theory: An Introduction, 1982.

[3] H. Saadat, Power System Analysis, McGraw-Hill, 1999.

[4] D.P. Kothari, I. Nagrath, Modern Power System Analysis, Tata McGraw-Hill Publishing Company, 2003.

[5] S. M. Abd-Elazim, E.S. Ali, Load frequency controller design of a two-area system composing of PV grid and thermal generator via Firefly Algorithm, Neural Comput. Appl. 30(2) (2018) 607–616.

[6] F. T. Tomy, R. Prakash, Load frequency control of a two-area hybrid system consisting of a grid-connected PV system and thermal generator, Technology 3(2) (2014) 4.

[7] R. K. Khadanga, A. Kumar, S. Panda, A novel modified Whale Optimization Algorithm for load frequency controller design of a two-area power system composing of PV grid and thermal generator, Neural Comput. Appl. 32(12) (2020) 8205 – 8216.

[8] P. Dahiya, A. K. Saha, Frequency regulation of interconnected power system using Black Widow Optimization, IEEE Access 10 (2022) 25219 – 25236.

[9] E. Çelik, N. Öztürk, E. H. Houssein, Influence of energy storage device on load frequency control of an interconnected dual-area thermal and solar photovoltaic power system, Neural Comput. Appl. 34(22) (2022) 20083 – 20099.

[10] V. Padiachy, U. Mehta, Novel fractional-order proportional-integral controller for hybrid power system with solar grid and reheated thermal generator, Solar 3(2) (2023) 298–321.

[11] P. Dash, L. C. Saikia, N. Sinha, Comparison of performances of several FACTS devices using Cuckoo Search Algorithm optimized 2DOF controllers in multi-area AGC, Int. J. Electr. Power Energy Syst. 65 (2015) 316–324.

[12] L. C. Saikia, J. Nanda, S. Mishra, Performance comparison of several classical controllers in AGC for multi-area interconnected thermal system, Int. J. Electr. Power Energy Syst. 33(3) (2011) 394 – 401.

[13] I. Koley, A. Datta, G. K. Panda, S. Debbarma, TLBO-optimised PIDD controller for coordinated control in a hybrid AC/DC microgrid, in: 2022 4th Int. Conf. Energy, Power and Environment (ICEPE), IEEE, 2022, 1 – 6.

[14] I. Koley, B. Sarkar, A. Datta, G. K. Panda, Load frequency control of a wind-energy-integrated multi-area power system with CSA-tuned PIDD controller, in: 2020 IEEE First Int. Conf. Smart Technologies for Power, Energy and Control (STPEC), IEEE, 2020, 1 – 6.

[15] A. Datta, G. Bhattacharya, D. Mukherjee, H. Saha, An efficient technique for controlling power flow in a single-stage grid-connected photovoltaic system, Sci. Iran. 21(3) (2014) 885 – 897.

[16] M. H. Amiri, N. Mehrabi Hashjin, M. Montazeri, S. Mirjalili, N. Khodadadi, Hippopotamus Optimization Algorithm: A novel nature-inspired optimization algorithm, Sci. Rep. 14(1) (2024) 5032.

[17] J. Kennedy, R. Eberhart, Particle Swarm Optimization, in: Proc. ICNN'95 – Int. Conf. Neural Networks, vol. 4, IEEE, 1995, 1942 – 1948.

[18] H. Eskandar, A. Sadollah, A. Bahreininejad, M. Hamdi, Water Cycle Algorithm – a novel metaheuristic optimization method for solving constrained engineering optimization problems, Comput. Struct. 110 (2012) 151 – 166.

[19] S. Mirjalili, S. M. Mirjalili, A. Lewis, Grey Wolf Optimizer, Adv. Eng. Softw. 69 (2014) 46 – 61.

[20] S. Ekinci, Ö. Can, M. Ş. Ayas, D. Izci, M. Salman, M. Rashdan, Automatic generation control of a hybrid PV–reheat thermal power system using RIME algorithm, IEEE Access 12 (2024) 26919 – 26930.

[21] A. Patel, A. Solegaonkar, Maximum power point tracking theorem by using solar photovoltaic panel, (n.d.).

[22] T. Santy, R. Natesan, Load frequency control of a two-area system consisting of a grid-connected PV system and diesel generator, Int. J. Emerg. Technol. Comput. Electron. 13(1) (2015) 456 – 461.

[23] A. Oshaba, E. S. Ali, S. M. Abd Elazim, PI controller design using ABC Algorithm for MPPT of PV system supplying DC motor pump load, Neural Comput. Appl. 28(2) (2017) 353 – 364.

[24] A. Oshaba, E. S. Ali, S. M. Abd Elazim, PI controller design for MPPT of photovoltaic system supplying SRM via BAT Search Algorithm, Neural Comput. Appl. 28(4) (2017) 651 – 667.

[25] M. T. Özdemir, D. Öztürk, Comparative performance analysis of optimal PID parameters tuning based on the optics-inspired optimization methods for automatic generation control, Energies 10(12) (2017) 2134.